Advanced Powder Technology xxx (xxxx) xxx

Contents lists available at ScienceDirect

Advanced Powder Technology

journal homepage: www.elsevier.com/locate/apt

Investigation of nanostructured FeNi hollow microspheres properties synthesized by ultrasonic spray pyrolysis

V.L. Kurichenko [a,*], E.V. Argunov [a], D.Yu. Karpenkov [a,b], E.A. Kolesnikov [a]

[a] National University of Science and Technology MISIS, Moscow 119049, Russia
[b] Lomonosov Moscow State University, Moscow 119991, Russia

ARTICLE INFO

Article history:
Received 9 December 2023
Received in revised form 15 April 2024
Accepted 24 April 2024
Available online xxxx

Keywords:
Nanostructured materials
Ultrasound spray pyrolysis
Iron-nickel alloy

ABSTRACT

In this work we studied properties of FeNi hollow nanostructured microspheres produced by ultrasonic spray pyrolysis technique. Specifically, we investigated how precursor solution (0.05–0.5 M) and reduction temperature (360–400 °C) influence properties of microspheres. By adjusting those values we were able to obtain samples with different microspheres diameter and crystallites size. Magnetic properties for the sample obtained from 0.1 M precursor and reduced at 400 °C were: saturation magnetization (M_S) of 130 emu/g, coercivity (H_C) of 87 Oe and Curie temperature (T_C) of 554 °C. Those values are higher than previously reported values in the literature for FeNi nanoparticles with equiatomic composition. Plotting relation matrix of various measured properties allowed us to evaluate different dependencies, making it possible to rationalize samples properties in a wider sense.

1. Introduction

Soft magnetic materials are materials that can be easily magnetized and demagnetized. Due to their properties, including low coercive force and high magnetic permeability, these materials have applications in areas where quick magnetization without energy loss is necessary (smartphones, PCs, electric generators, aerospace equipment etc.) [1].

One of the example of such materials is the Fe-Ni (FeNi) alloy. This alloy is interesting not only due to the usage in soft materials applications [2], but also as a precursor for FeNi $L1_0$ phase, which was shown in the literature as a perspective rare-earth free hard magnetic material [3–5]. In order to fully utilize the potential of this alloy, the optimization of its properties is needed, as it was shown that by changing the morphological properties of this alloy it is possible to alter its magnetic properties [6–8].

Traditionally, this alloy is produced by classical metallurgical methods, such as induction and arc melting. However, various studies were conducted to obtain this phase using alternative methods, such as mechanical grinding [9], sol–gel method [10], and spray pyrolysis [11–13,7]. Among these methods, spray pyrolysis technique is particularly noteworthy due to its simplicity, low cost of precursors, high yield of reaction products and ability to obtain particles with spherical shape, which is crucial for maximizing magnetic properties [14]. Obtaining the powders in the initially spherical form makes it possible to use them without additional step of spheroidization [15,16] for creating materials with complex geometries by using such techniques as Selective Laser Melting (SLM), Selective Laser Sintering (SLS) or additive manufacturing, where the spherical particle shape is critical [7,17].

Spray pyrolysis technique can have one or multiple stages. In one-staged variant the droplets are transferred through the reaction zone by reducing gas carrier, such as hydrogen (H_2) [13,11]. However, this variant can be dangerous due to usage of hydrogen gas at elevated temperatures, which are required for successful salts decomposition [11]. Another variant is obtaining the oxide particles first and then reducing them in the hydrogen atmosphere [18,8]. In that case it is possible to perform heat treatment in reduction atmospheres at lower temperatures, thus allowing more control on morphological properties of metallic particles.

Additionally, careful optimization of pyrolysis technique parameters allows obtaining hollow microspheres with precisely adjusted composition and morphology (spheres diameter, as well as size of the nanoparticles that construct the sphere) [24], making the obtained results reproducible. The interplay between these two parameters can lead to changes in properties of such materials, e.g. magnetic and optical ones [20,19].

* Corresponding author.
E-mail address: vkurichenko@misis.ru (V.L. Kurichenko).

https://doi.org/10.1016/j.apt.2024.104461

Please cite this article as: V.L. Kurichenko, E.V. Argunov, D.Yu. Karpenkov et al., Investigation of nanostructured FeNi hollow microspheres properties synthesized by ultrasonic spray pyrolysis, Advanced Powder Technology, https://doi.org/10.1016/j.apt.2024.104461

Thus, the aim of this article was to optimize the two-staged spray pyrolysis technique for production of FeNi hollow nanostructured microspheres. For that, the particles were produced from different precursor solutions and reduced in hydrogen atmosphere at different temperatures.

2. Experimental

2.1. Hollow microspheres production

The following chemicals were used as precursors for obtaining nanostructured Fe-Ni-O microspheres by spray pyrolysis: iron (III) nitrate 9-aqueous $Fe(NO_3)_3{\cdot}9H_2O$, analytical grade; nickel(II) nitrate 6-aqueous $Ni(NO_3)_2{\cdot}6H_2O$, analytical grade; distilled water.

Three different concentrations of solutions were used in the work: 0.05, 0.1, and 0.5 M. The concentration of the components was calculated based on the composition of the metal product Ni:Fe = 1:1. The starting precursors, after being added to water, were thoroughly mixed and filtered using filter paper.

At the next stage, the spray pyrolysis process was carried out using ultrasonic generator with 1.7 MHz frequency. It was shown in the literature that using higher frequency yields particles with smaller diameter [21,22]. The generated steam entered the working zone of the tube furnace at a temperature of 1000 °C. This temperature was chosen because it was shown that this temperature is optimal in terms of the morphology of the resulting microspheres [11]. The pyrolysis of iron and nickel nitrates proceeds according to the chemical reactions [23]:

$$4Fe(NO_3)_3 \cdot 9H_2O \rightarrow 2Fe_2O_3 + 3O_2 + 12NO_2 + 36H_2O \quad (1)$$

$$2Ni(NO_3)_2 \cdot 6H_2O \rightarrow 2NiO + O_2 + 4NO_2 + 12H_2O \quad (2)$$

In the high temperature zone, the following physical phenomena simultaneously occur with the droplet: solvent evaporation from the droplet surface, solvent vapor diffusion from the droplet, droplet shrinkage, droplet temperature change, diffusion of the solute to the droplet center [24]. The powders collected on the filters were extracted and subsequently subjected to the process of reduction in hydrogen flow at various temperatures. The reduction can be described by the chemical reactions:

$$FeNiO + H_2 \rightarrow FeNi + H_2O \quad (3)$$

To prevent oxidation of the samples, passivation of their surface was carried out by using technical nitrogen, which contains a small amount of oxygen ($< 1\%$).

2.2. Characterization

The studies of dehydration processes were carried out using differential scanning calorimetry and thermogravimetry methods on SDT Q-600 analyzer. The process of dehydration of the powders was conducted under conditions of linear heating at a rate of 20 °C/min in a hydrogen atmosphere in the temperature range from 26 °C to 690 °C. The phase composition of the samples was studied on a Difrey-401 X-ray powder diffractometer. The measurements were carried out with Cr Kα radiation with 2.2909 Å wavelength. The morphology and chemical composition of the samples were examined using a Tescan Vega 3SB scanning electron microscope equipped with an Oxford Instruments Advanced energy dispersive X-ray microanalyzer. The samples were also examined on a Raman confocal microscope (Raman spectroscopy) Thermo DXR (USA), with 532 and 732 nm wavelength. The specific surface area was studied on a NOVA 1200 specific surface analyzer (USA). The field dependencies M(H) of the samples were obtained using vibrating sample magnetometer (VSM) LakeShore 7404.

3. Results

3.1. Choosing the reduction temperatures

As was pointed in introduction, the objective of this work is to optimize the process of obtaining hollow nanostructured FeNi microspheres by spray pyrolysis. The process of reduction to a metallic state is an important step in material synthesis that will determine the size of the resulting nanoparticles, which form the microsphere. If too high a temperature is used, sintering of the particles and, consequently, degradation of their properties is possible [25]. If the reduction temperature is insufficient, oxide phases may remain in the sample, which will also adversely affect the final properties [26]. In order to determine the temperature range in which the optimization of the sample preparation process will be performed, a thermogravimetric analysis was carried out in a reducing atmosphere. Fig. S2 shows the measurement results from which the reduction temperatures of interest were selected, specifically 360, 380 and 400 °C. At the next stage, all samples were reduced at these temperatures for 1.5 h.

3.2. Phase composition analysis

After reduction, phase analysis of the samples was carried out. X-ray diffraction (XRD) patterns after Rietveld refinement are presented in Supplementary (Figs. S3–S6). Fig. 1 shows XRD patterns of a sample obtained at a concentration of 0.1 M. It is seen that before reduction the sample consisted of the oxide phases (NiO and $NiFe_2O_4$). In the sample reduced at 360 °C small amount of oxide phases are still present, which tends to decrease when increasing the reduction temperature. Results of XRD quantitative phase analysis after Rietveld refinement are shown in Tables S1 and S2 for the initial samples and the reduced samples, respectively. For all concentrations in the reduced samples, a mixture of the fcc phases of FeNi and Fe_3O_4 is observed. For a sample obtained from a solution with 0.1 M concentration, the content of the oxide phase is minimal for all reduction temperatures. In order to confirm the phase composition of the samples before and after reduction, Raman spectroscopy studies were also carried out, since it allows differentiating between oxide phases (e.g. $NiFe_2O_4$ and Fe_3O_4, which are close on the XRD patterns [27]). Fig. S7 shows the Raman spectra of the samples, which confirms that Fe_3O_4 phase is presented in the sample after reduction.

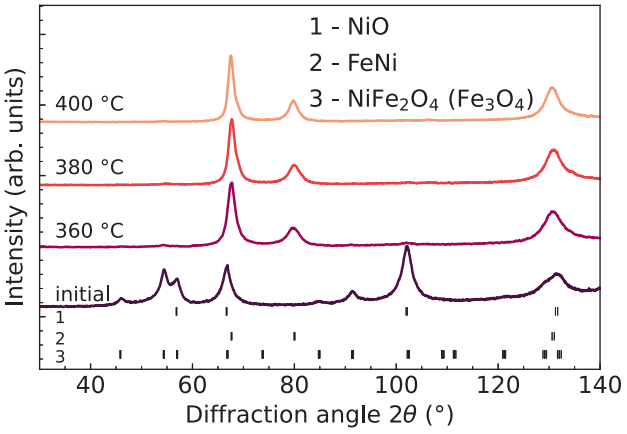

Fig. 1. X-ray diffraction patterns of a sample obtained at a precursor concentration of 0.05 M and reduced at different temperatures.

3.3. Morphological properties

The size of the coherent scattering regions (CSR) of all samples was also calculated using the Debye–Scherrer formula. The results are presented in Table S4. Typical trend is seen that the CSR size increases with reduction temperature [26].

At the next stage, the morphology of FeNi particles was studied by scanning electron microscopy (SEM). Fig. S8 shows microphotographs of the initial sample, where hollow microstructure of the samples can be seen. Figs. S9–S11 show microphotographs of all samples. Fig. 2 shows microphotographs of the 0.1 M sample reduced at different temperatures. It can be seen that the particles have a spherical shape, which is expected for this technique. To describe the size characteristics of spherical FeNi particles, it is necessary to study the size distributions of the particles. Fig. S12 shows histograms of the respective distributions, as well as average size of the spheres. For all temperatures, a decrease in the average size of the spheres is observed with a decrease in the concentration of the precursor solution, which agrees with the literature [21].

At the same time, if we consider samples of the same precursor concentration reduced at different temperatures, it is seen that in terms of smaller particle sizes the optimal reduction temperature is 380 °C. However, it is expected that there should not be any reduction temperature dependence of the particle diameters, as it should only affect crystalite sizes (see Table S4), so this change in diameter should be attributed to other reasons.

To additionally investigate sintering in the particles and evaluate the change in the pore volume in the particles, a study was carried out by low-temperature nitrogen adsorption technique. This allowed us to estimate the pore size distribution. The data obtained are shown in Fig. S13. The results showed that with increasing the reduction temperature, the pore size distribution shifts to the right, meaning that smaller pores are eliminated [28]. However, no dependence on the concentration of precursor solution was found.

3.4. Magnetic properties

At the next stage, the magnetic properties of all samples were studied. Supplementary materials contain all the data that was gathered from the samples: Fig. S14 shows the hysteresis loops. Fig. S15 shows temperature dependence of magnetization. Fig. S15 shows magnetic properties, extracted from the curves mentioned above. Below, Fig. 3 shows data for the sample obtained from 0.1 M precursor solution. Two distinct trends are observed on the figure: decrease of the Curie temperature and increase of saturation magnetization for the samples, reduced at higher temperatures. However, is seen that coercivity of this sample is not changing significantly as opposed to other concentrations (see Fig. S16a). However, one should consider not only the reduction temperature when trying to describe these dependencies, which we will address in the next chapter.

It is difficult to compare the properties of our samples with the literature, since there is not many articles that were investigating magnetic properties of FeNi with equiatomic composition obtained by ultrasonic spray pyrolysis. E.g. equiatomic FeNi was obtained, but magnetic properties were not measured [11,2,13], or the magnetic properties were measured, but the samples had $Fe_{25}Ni_{75}$ composition [7]. Thus, we can only compare our properties with equiatomic FeNi, obtained by other methods. If we consider the sample that was obtained from 0.1 M precursor solution and reduced at 400 °C, it has the following magnetic properties: saturation magnetization (M_S) of 130 emu/g, coercivity (H_C) of 87 Oe and Curie temperature (T_C) of 554 °C. The value of Curie temperature is higher than the value for the bulk samples (500 °C) [29]. The values of H_C and M_S are higher than the values obtained in our previous work via chemical precipitation method (50 Oe and 80 emu/g, respectively) [5]. By means of hydrazine reduction the authors obtained FeNi with H_C = 50 Oe and M_S = 130 emu/g [30]. In other work, the authors used auto-combustion and hydrogen reduction for synthesis of equiatomic FeNi and obtained the values of 26.5

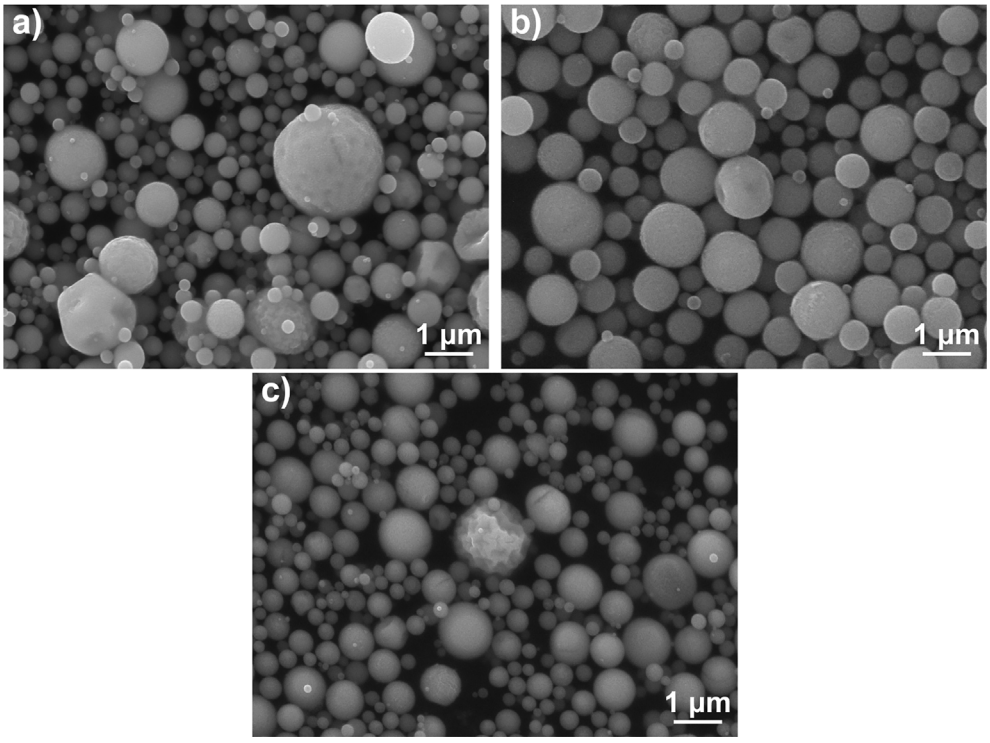

Fig. 2. SEM microphotographs of the 0.1 M sample reduced at different temperatures: a) 360 °C, b) 380 °C, c) 400 °C.

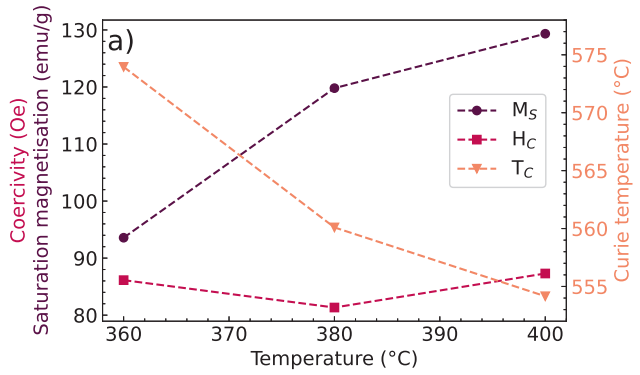

Fig. 3. Temperature dependence of magnetic properties of the sample obtained from 0.1 M precursor solution (saturation magnetization, coercivity and Curie temperature).

Oe and 108.6 emu/g, respectively [31]. Thus, measured magnetic properties are the same of higher as compared to the values reported in literature. However, there is still room for improvement of the samples properties, e.g. by reducing crystallites size up to single-domain size it is possible to improve coercivity [32]. It was shown for FeNi nanoparticles that reducing crystallites size allowed to obtain coercivity up to 246 Oe [33].

4. Discussion

Different techniques and methods were used to characterize the samples. In order to see the wider picture of solution concentration and reduction temperature dependence on the properties of the samples, we created interactive graph by using *plotly* library in Python. The interactive graph in *.html* format can be found in the Supplementary material of online version of the manuscript. In the following text we will discuss some trends that are present on this graph and try to rationalize all the resulting properties. Here we will present only parts of the dependencies that we found relevant for the article. For the other dependencies the reader is referred to the interactive graph.

4.1. Composition

At first, let's consider temperature dependence on the composition. In the first column, which corresponds to temperature dependence of the properties, there is a definitive trend seen that the percentage of FeNi phase is increasing with increased reduction

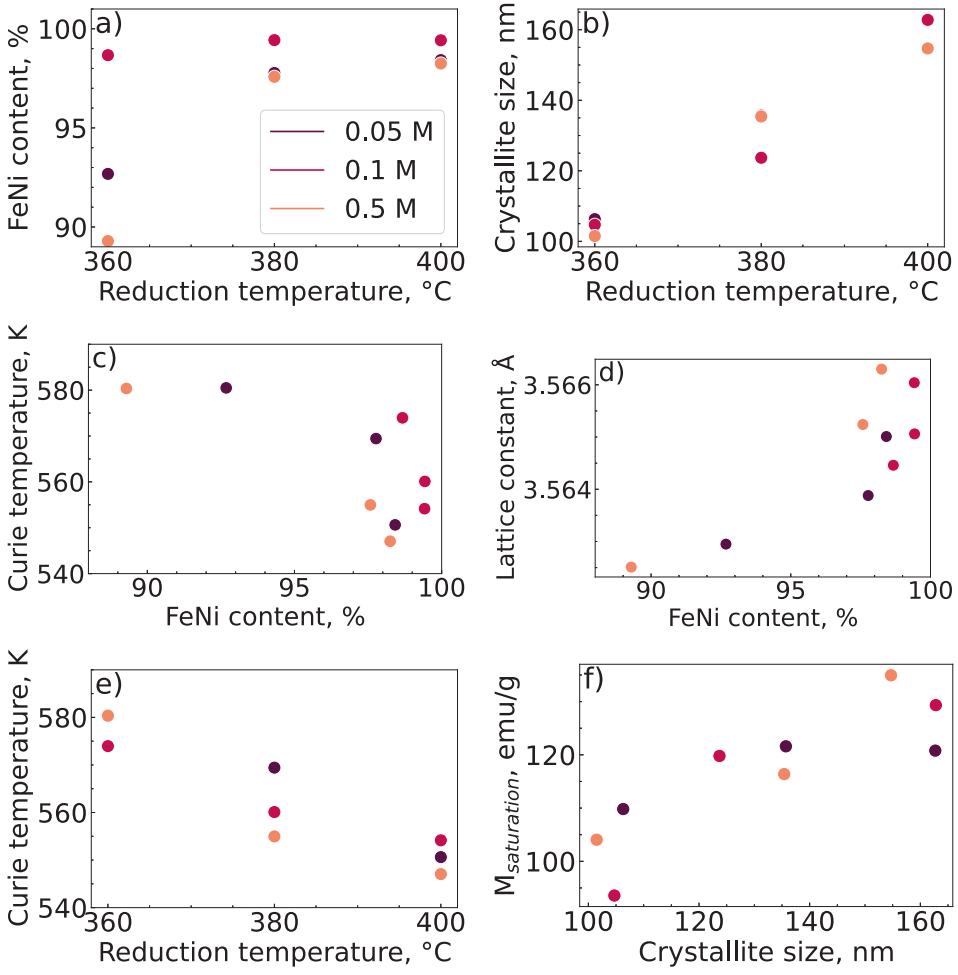

Fig. 4. Dependencies: a) FeNi content vs reduction temperature, b) crystallites size vs reduction temperature, c) Curie temperature vs FeNi content, d) Lattice constant vs FeNi content, e) Curie temperature vs reduction temperature, f) Saturation magnetization vs crystallites size.

temperature (Fig. 4a), which is in agreement with the results of Rietveld analysis (see Table S2).

4.2. Morphology

Secondly, we can consider morphological properties. Mean diameter of the spheres seems to not scale linearly with the temperature. Schrerrer diameter, calculated from XRD patterns shows expected trend of increase with the temperature (Fig. 4b). BET diameter is also increasing with the temperature, which is expected as crystallites size grow with reduction temperature.

4.3. Magnetic properties

Finally, we will refer to the magnetic properties of the samples. If we look at the second column, which corresponds to dependence of FeNi percentage on properties, one of the trends that is observed is the decrease of T_C with increase of FeNi content in the sample (Fig. 4c). The results of Raman spectroscopy (see Fig. S7) revealed that iron oxide phases are present in samples after reduction, thus, the iron-nickel phase in the sample will have lower iron content. This is also confirmed by small increase of lattice constant with increased iron content (see Table S3 and Fig. 4d), which was reported in the literature [34]. Also, it was shown that in iron-nickel alloys near equiatomic composition Curie temperature is decreasing with increased Fe content [35], which explains observed results. Decrease of the Curie temperature with reduction temperature (Fig. 4e) can be explained by the same reasons.

In order to validate that the reason for the change in Curie temperature is the composition, but not the morphology of the particles, (crystallites size affect Curie temperature values [36]) we performed magnetic simulations, which are presented in Supplementary in Section 6. The simulations revealed that Curie temperature should not be dependent on the particle size in the investigated region.

Another trend that is observed is almost linear dependence of saturation magnetization of the samples with the increase of reduction temperature. This trend can be explained by the interplay between increased crystallinity of the sample (Fig. 4f) [37] and the FeNi content of the sample, which means that there is an increased Fe content, having higher magnetization as compared to Ni [38].

5. Conclusion

Various investigation techniques were used on the FeNi hollow microspheres, which were obtained via ultrasonic spray pyrolysis method. Different precursor solutions and reduction temperatures were used, which allowed to argue about optimal parameters for magnetic properties optimization. It was shown that the samples have magnetic properties that are mostly higher than previously reported values for FeNi nanostructured materials. Additionally, we propose further improvement of the properties, e.g. by reducing crystallites size of the particles.

Plotting results of the investigation on the interactive graph allowed us to find different dependencies, explaining the properties of our samples. Hence, when using hollow nanostructured microspheres (and other materials) one should not only consider how one property depends on another (e.g. Curie temperature on the reduction temperature) but also try to rationalize the full picture of the sample properties in terms of its phase composition, morphology etc.

Data availability

The data that support the findings of this study are available from the corresponding author, V.K., upon reasonable request.

CRediT authorship contribution statement

L. K.V.: Conceptualization, Methodology, Investigation, Formal analysis, Data curation, Writing – original draft, Visualization, Writing – review & editing. **V. A.E.:** Methodology, Investigation, Writing – original draft. **Yu. K.D.:** Investigation. **A. K.E.:** Conceptualization, Methodology, Investigation, Formal analysis, Supervision, Writing – review & editing.

Declaration of competing interest

The authors declare that they have no known competing financial interests or personal relationships that could have appeared to influence the work reported in this paper.

Acknowledgements

The study was funded by the Ministry of Science and Higher Education of the Russian Federation under the strategic academic leadership program "Priority 2030" at NUST MISIS. We acknowledge Muratov D.S. for the help with methodology and investigation.

Appendix A. Supplementary data

Supplementary data associated with this article can be found, in the online version, at https://doi.org/10.1016/j.apt.2024.104461.

References

[1] Akihisa Inoue, Fanli Kong, Soft magnetic materials, in: Abdul-Ghani Olabi, (Ed.), Encyclopedia of Smart Materials, Elsevier, Oxford, 2022, pp. 10–23.
[2] Eka Lutfi Septiani, Jun Kikkawa, Kiet Le Anh Cao, Tomoyuki Hirano, Nobuhiro Okuda, Hiroyuki Matsumoto, Yasushi Enokido, Takashi Ogi, Dc bias characteristic enhancement of the powder core by using densified submicron sized feni particles through spray pyrolysis, J. Mater. Chem. C 10 (2022).
[3] Sho Goto, Hiroaki Kura, Eiji Watanabe, Yasushi Hayashi, Hideto Yanagihara, Yusuke Shimada, Masaki Mizuguchi, Koki Takanashi, Eiji Kita, Synthesis of single-phase l10-feni magnet powder by nitrogen insertion and topotactic extraction, Scientific Rep. 7 (2017) 13216.
[4] N. Bordeaux, A.M. Montes-Arango, J. Liu, K. Barmak, L.H. Lewis, Thermodynamic and kinetic parameters of the chemical order–disorder transformation in l10 feni (tetrataenite), Acta Mater. 103 (2016) 608–615.
[5] Vladislav L. Kurichenko, Dmitriy Yu Karpenkov, Alexey Yu Karpenkov, Marina B. Lyakhova, Vladimir V. Khovaylo, Synthesis of feni tetrataenite phase by means of chemical precipitation, J. Magn. Magn. Mater. 470 (2019).
[6] Tien Hiep Nguyen, Gopalu Karunakaran, Yu V. Konyukhov, Nguyen Van Minh, D. Yu Karpenkov, I.N. Burmistrov, Impact of iron on the fe–co–ni ternary nanocomposites structural and magnetic features obtained via chemical precipitation followed by reduction process for various magnetically coupled devices applications, Nanomaterials 11 (2021).
[7] H.C. Jang, S.H. Ju, Y.C. Kang, Characteristics of fine size fe-ni alloy powders directly prepared by spray pyrolysis, Met. Mater. Int. 16 (2010).
[8] Pei Kai Hsu, Shih Yun Chen, Ji Nan Cheng, Jenn Ming Song, Kiyokazu Yasuda, Hollow iron submicron spheres with strong ferromagnetism, Mater. Lett. 308 (2022).
[9] G. Gonzalez, A. Sagarzazu, D. Bonyuet, L. D'Angelo, R. Villalba, Solid state amorphisation in binary systems prepared by mechanical alloying, J. Alloy. Compd. 483 (2009).
[10] Cássio Morilla Dos Santos, Adanny Filipe Nogueira Martins, Bruna Carolina Costa, Thiago Soares Ribeiro, Tiago Pinheiro Braga, João Maria Soares, José Marcos Sasaki, Synthesis of feni alloy nanomaterials by proteic sol-gel method: Crystallographic, morphological, and magnetic properties, J. Nanomater. 2016 (2016).
[11] Eka Lutfi Septiani, Jun Kikkawa, Kiet Le Anh Cao, Tomoyuki Hirano, Nobuhiro Okuda, Hiroyuki Matsumoto, Yasushi Enokido, Takashi Ogi, Direct synthesis of submicron feni particles via spray pyrolysis using various reduction agents, Adv. Powder Technol. 32 (2021).

[12] S. Eroglu, S.C. Zhang, G.L. Messing, Synthesis of nanocrystalline ni-fe alloy powders by spray pyrolysis, J. Mater. Res. 11 (1996).
[13] Sebahattin Gurmen, Burcak Ebin, Srecko Stopic, Bernd Friedrich, Nanocrystalline spherical iron-nickel (fe-ni) alloy particles prepared by ultrasonic spray pyrolysis and hydrogen reduction (usp-hr), J. Alloy. Compd. 480 (2009).
[14] Peter Majeric, Rebeka Rudolf, Advances in ultrasonic spray pyrolysis processing of noble metal nanoparticles-review, Materials 13 (2020).
[15] M. Hossein Sehhat, Austin T. Sutton, Chia-Hung Hung, Ben Brown, Ronald J. O'Malley, Jonghyun Park, Ming C. Leu, Plasma spheroidization of gas-atomized 304l stainless steel powder for laser powder bed fusion process, Mater. Sci. Addit. Manuf. 1 (2022).
[16] M. Hossein Sehhat, Jackson Chandler, Zane Yates, A review on icp powder plasma spheroidization process parameters, 2022.
[17] A.K. Mazeeva, M.V. Staritsyn, V.V. Bobyr, S.A. Manninen, P.A. Kuznetsov, V.N. Klimov, Magnetic properties of fe–ni permalloy produced by selective laser melting, J. Alloy. Compd. 814 (2020).
[18] Andrey Yudin, Nadezda Shatrova, Bekzod Khaydarov, Denis Kuznetsov, Ella Dzidziguri, Jean Paul Issi, Synthesis of hollow nanostructured nickel oxide microspheres by ultrasonic spray atomization, J. Aerosol Sci. 98 (2016).
[19] Debasish Sarkar, Arup Ghosh, Rupali Rakshit, Kalyan Mandal, Magnetic properties of fe3o4 nano-hollow spheres, J. Magn. Magn. Mater. 393 (2015).
[20] Quan Lin Ye, Hirofumi Yoshikawa, Kunio Awaga, Magnetic and optical properties of submicron-size hollow spheres, 2010.
[21] Srecko Stopic, Felix Wenz, Tatjana Volkov Husovic, Bernd Friedrich, Synthesis of silica particles using ultrasonic spray pyrolysis method, Metals 11 (2021).
[22] Richard L. Peskin, Roland J. Raco, Ultrasonic atomization of liquids, J. Acoust. Soc. Am. 35 (1963).
[23] Baicheng Zhang, Nour Eddine Fenineche, Hanlin Liao, Christian Coddet, Studies of magnetic properties of permalloy (fe30%ni) prepared by slm technology, J. Magn. Magn. Mater. 324 (2012).
[24] S. Rahemi Ardekani, Alireza Sabour Rouh Aghdam, Mojtaba Nazari, Amir Bayat, E. Yazdani, Esmaiel Saievar-Iranizad, A comprehensive review on ultrasonic spray pyrolysis technique: Mechanism, main parameters and applications in condensed matter, J. Anal. Appl. Pyrol. 141 (2019).
[25] Yang Liu, Tao Sun, Gang Dong, Shuai Zhang, Kaili Chu, Xingrui Pu, Hongjiang Li, Xiang Liu, Dependence on sintering temperature of structure, optical and magnetic properties of la0.625ca0.315sr0.06mno3 perovskite nanoparticles, Ceram. Int. 45 (2019).
[26] Mikio Kishimoto, Eiji Kita, Hideto Yanagihara, Structure and magnetic properties of nitrides in feni and fenico alloy particles synthesized via co-precipitation, reduction, and nitriding, J. Magn. Magn. Mater. 548 (2022).
[27] B. Sahu, U.K. Panigrahi, C.J. Sheppard, A.R.E. Prinsloo, P. Mohanty, P. Mallick, Structural and magnetic characteristics of nio/nife2o4/a-fe2o3 nanocomposite, Mater. Chem. Phys. 302 (2023).
[28] Jai Sung Lee, Joon Phil Choi, Geon Yong Lee, Consolidation of hierarchy-structured nanopowder agglomerates and its application to net-shaping nanopowder materials, Materials 6 (2013).
[29] Michael Wack, Michael Volk, Qingguo Wei, Magnetic properties of the iron–nickel system: pressure, composition, and grain size, 2018.
[30] Norhan Nady, Noha Salem, Marwa A.A. Mohamed, Sherif H. Kandil, Iron-nickel alloy with starfish-like shape and its unique magnetic properties: effect of reaction volume and metal concentration on the synthesized alloy, Nanomaterials 11 (2021).
[31] Neera Singh, Shyam Sharma, Om Parkash, Devendra Kumar, Synthesis and characterization of nanocrystalline fe(100–x)ni(x) alloy powders by auto-combustion and hydrogen reduction, J. Mater. Eng. Perform. 28 (2019).
[32] Ji Sung Lee, Jin Myung Cha, Ha Young Yoon, Jin Kyu Lee, Young Keun Kim, Magnetic multi-granule nanoclusters: a model system that exhibits universal size effect of magnetic coercivity, Scientific Rep. 5 (2015).
[33] Xian Wen Wei, Guo Xing Zhu, Ju Hong Zhou, Hui Qun Sun, Solution phase reduction to fe-ni alloy nanostructures with tunable shape and size, Mater. Chem. Phys. 100 (2006).
[34] E.A. Owen, E.L. Yates, A.H. Sully, An x-ray investigation of pure iron-nickel alloys. Part 4: the variation of lattice-parameter with composition, Proc. Phys. Soc. (1937) 49.
[35] Qingguo Wei, Stuart Alan Gilder, Bernd Maier, Pressure dependence on the remanent magnetization of fe-ni alloys and ni metal, Phys. Rev. B 90 (2014).
[36] Ling fei Cao, Dan Xie, Ming xing Guo, H.S. Park, T. Fujita, Size and shape effects on curie temperature of ferromagnetic nanoparticles, Trans. Nonferrous Met. Soc. China (English Edition) 17 (2007).
[37] Saroj Dhaka, Sudesh Kumar, K. Poonia, Vidyadhar Singh, Kapil Dhaka, H.S. Mund, Effect of annealing temperature on structural and magnetic properties of nano-cobalt ferrite, J. Mater. Sci.: Mater. Electron. 32 (2021).
[38] Girfan Shamsutdinov, Peng Zhao, Sreenivas Bhattiprolu, Ji Cheng Zhao, Boris Nadgorny, Magnetization–structure–composition phase diagram mapping in co-fe-ni alloys using diffusion multiples and scanning hall probe microscopy, Scientific Rep. 12 (2022).